Transport study of percolation modes in the mixed-phase manganites

Qing-li Zhou, Kui-juan Jin,* Kun Zhao, Dong-yi Guan, Hui-bin Lu, Zheng-hao Chen, and Guo-zhen Yang
Beijing National Laboratory for Condensed Matter Physics, Institute of Physics, Chinese Academy of Sciences, P.O. Box 603, Beijing 100080, China

(Received 11 July 2005; revised manuscript received 27 September 2005; published 30 December 2005)

Based on the phase separation scenario, cluster percolation mode is introduced to simulate the percolative conduction of $La_{0.9}Te_{0.1}MnO_3$ and $La_{2/3}Ca_{1/3}MnO_3$ thin films with the abrupt metal-to-insulator transition of resistivity, while standard percolation mode, which seems to work well for $La_{0.9}Te_{0.1}MnO_3$ bulk with smooth transition, fails in it. The agreement between the simulation and the experimental data reveals that the sizes of the paramagnetic domains in the films increases, but the number of those domains does not change with the increased temperature. This process is very different from the case in the bulk, where the domain sizes almost remain unchanged and the domain number increases with the increased temperature. The present results also further verify that phase separation plays a crucial role in the transport process and the size of coexisting phase may be related to the size of the crystal grains.

DOI: 10.1103/PhysRevB.72.224439 PACS number(s): 75.47.Lx, 64.75.+g, 84.37.+q, 64.60.Ak

I. INTRODUCTION

Perovskite manganites are currently under considerable experimental and theoretical investigation due to the observation of colossal magnetoresistance (CMR).[1] Those manganites usually have a metal-to-insulator transition (MIT) accompanied by a simultaneous phase-to-phase transition, such as a ferromagnetic (FM) metallic to paramagnetic (PM) insulating transition[2–4] or a FM to charge ordering (CO) transition.[5,6] Furthermore, when applying an external magnetic field H, the temperature T of the MIT will move to a higher value and the resistivity will decrease correspondingly. However, these properties remain a matter of speculation. The double exchange model (DE),[7] describing the hopping of the e_g electrons in the system and the electron-lattice coupling[8] leading to the Jahn-Teller (J-T) polaron formation, seem not to be sufficient for explaining the phase transition and the enormous magnitude of magnetoresistance for some materials such as $La_{5/8-y}Pr_yCa_{3/8}MnO_3$.[4]

A promising description is the percolative transport through the mixed-phase domains, suggesting that the manganites have a strong tendency toward phase separation with intrinsic inhomogeneity. Experimentally, phase separation phenomenon has been observed in many systems of manganites,[5,9–11] such as the coexistence of PM and FM phases on a large submicrometer scale just below T_c in $La_{0.73}Ca_{0.27}MnO_3$ thin film.[12] Furthermore, it is found that the resistivity of thin film usually has a rather abrupt character change near the MIT[13] compared with that of bulk material.[2,4,5,14,15] Theoretically, Mayr *et al.*[16] used a random resistor network to study the resistivity of manganite and obtained qualitative agreement with some experiments. Burgy *et al.*[17] further proposed a semiphenomenological description based on coexisting clusters with smooth surfaces to explain the abrupt percolative transition and even first order discontinuities of Mn oxides. However, those theoretical studies are of qualitative simulations, lacking in the quantitative investigation. Therefore, based on the standard percolation mode,[18] we have simulated and obtained quantitative agreement with our experimental data for $La_{0.96}Te_{0.04}MnO_3$ bulk.[19] Although standard percolation is a good random statistical model for a variety of systems, this percolation mode seems unsuitable to simulate the abrupt change in the resistivity near the transition of the thin films. In the present work, the cluster percolation mode is introduced to depict the electrical transport in $La_{0.9}Te_{0.1}MnO_3$ and $La_{2/3}Ca_{1/3}MnO_3$ thin films with abrupt MIT, as well as for standard percolation for $La_{0.9}Te_{0.1}MnO_3$ bulk with smooth transition. The obtained results indicate that cluster percolation can show more of the physical mechanism of the thin film than the standard percolation. It shows the PM cluster sizes of the film increase, but the cluster number is nearly unchanged with T. In Sec. II, the random network model, the corresponding method for calculating resistivity, and two different percolation modes are described briefly. In Sec. III, the simulated results and the corresponding experimental data are displayed, including the snapshots of the phase transition process for standard and cluster percolations. A discussion of results is presented in Sec. IV and the main conclusions are given in Sec. V.

II. MODEL AND METHOD

The main concept of the random network model is that the system, i.e., a two-dimensional (2D) $N\times N$ matrix, is composed of two phases with different conductive properties. One is the FM metallic phase with resistance $R_M(T)$, the other is the PM insulating phase with resistance $R_I(T)$. The total effective resistance R_{eff} is determined by the parallel connection of $R_M(T)$ and $R_I(T)$. A quantity f, defined as f= (the number of FM lattice sites)/(the total number of lattice sites), represents the fraction of FM metallic sites $(0\leqslant f\leqslant 1)$. Naturally, the fraction of PM insulating sites is $(1-f)$. As a matter of fact, f is a function of not only T, but also of H.[19] Since the metallic component triggered by ferromagnetism is sensitive to the temperature, the fraction of FM metallic phases is assumed to be proportional to the T-dependent magnetization.[20] Mayr *et al.* have pointed out that f should decrease with the increased T and change rap-

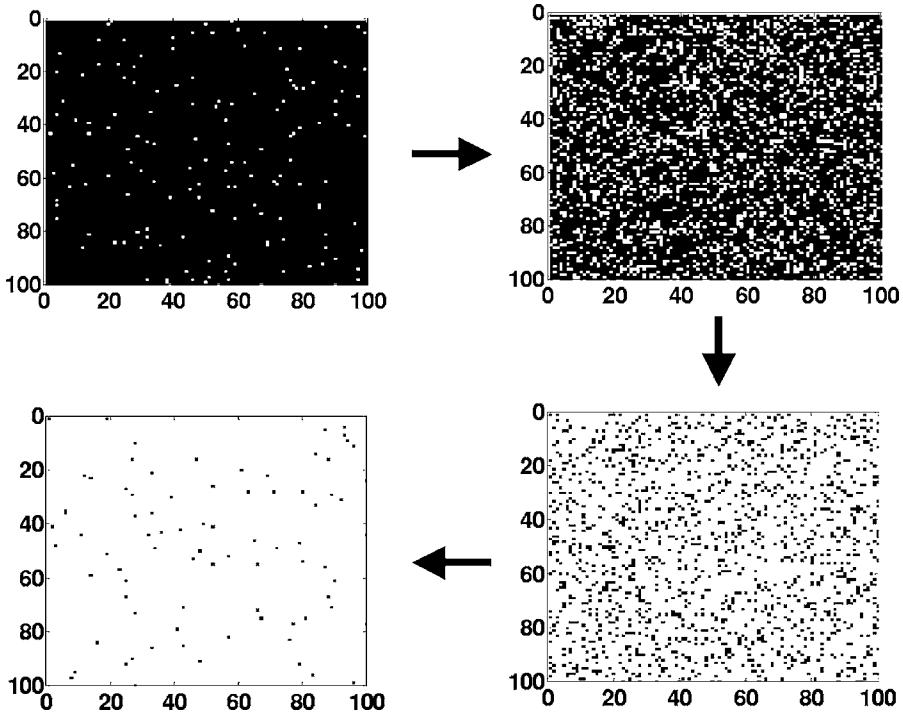

FIG. 1. Simulated process of standard percolation from low-T FM (black) to high-T PM (white) phase transition in the mixed-phase description in a 100×100 matrix. The arrows indicate the warming process.

idly near T_c. They have also found that the qualitative results using several functions to describe the FM fraction f are similar, showing agreement with some experiments.[16] For simplification, we use the Fermi distribution-like function to describe f because the shape of this function is very similar to the T-dependent magnetization obtained from the experimental data. The FM metallic fraction f is in the form of $f=1/\{1+B\exp[A(T-T_c+T_{MI}^0-T_{MI}^H)]\}$, where T_{MI}^H and T_{MI}^0 are the MIT temperature with and without H, respectively. We assume this function is adaptive in the whole studied temperature region. In the formula of f, parameter B is related to the critical concentration f_0 for percolation, satisfying $B=(1-f_0)/f_0$. In Ref. 21, it is mentioned that this percolation threshold value f_0 is 0.5 in 2D. In our simulation, f_0 is 0.5 or changes to 0.45 for fitting. Parameter A reflects the temperature width for the coexisting phases, being the result of a fitting procedure.

To calculate $R_M(T)$ and $R_I(T)$, we assume $\rho_m(T)=\rho_{m0}+\rho_{m1}T^2+\rho_{m2}T^{4.5}$ and $\rho_i(T)=\rho_{i0}\exp[E_0/(k_BT)]$ are the T-dependent resistivities for each FM site and PM site, respectively. ρ_{m0} is the residual resistivity at $T\sim0$ K, the T^2 term indicates the electron scattering[22] with the coefficient ρ_{m1}, and the $T^{4.5}$ term denotes the magnon scattering involving the phonon scattering[23] with the coefficient ρ_{m2}. The coefficient ρ_{i0} is the high-T residual resistivity, E_0 is the activation energy, and k_B represents the Boltzmann constant.[24,25] Although there are five parameters in FM and PM resistivities, in fact, the low-T residual resistivity ρ_{m0} and the high-T residual resistivity ρ_{i0} can be obtained directly from the experimental data of the low-T and high-T regions, respectively. In the simulation procedure, those two parameters remain unchanged, so only three parameters $(\rho_{m1},\rho_{m2},E_0)$ need to be adjusted. Using the Breadth First Traversal algorithm,[26] the path lengths of the metallic and insulating domains are found to calculate $R_M(T)$ and $R_I(T)$, respectively. The effective resistivity is then obtained according to the size of the sample.

With the temperature evolution, the distribution of FM and PM components can be accomplished by standard percolation and cluster percolation modes. In the standard percolation mode, the occupation of the square is random; that is, each square is occupied by a FM or PM site independent of the occupation status of its neighbors. At a fixed initial low T, each square in the matrix is occupied randomly by an FM site with the probability $f(T)$. With increasing T, FM metallic squares are randomly selected to convert into PM insulating squares. However, in the cluster percolation mode, the occupation of the square is correlated with the status of its neighbors. When T is increased, only those FM sites which have at least one PM neighbor can turn into PM squares, resulting in the growth of the PM domain. The main difference between these two modes lies in the variation of domain size and domain number under the temperature evolution. During the warming process, cluster percolation demonstrates a process that the PM domain size increases but the domain number stays unchanged, while standard percolation embodies a process in which the domain size is nearly unchanged but the domain number increases.

III. RESULTS

To show the mixed-phase percolative conduction from the phenomenological view, the standard percolation scenario obtained from the simulation is illustrated in Fig. 1 for the transition from the FM phase to PM phase with the increased T. The small dark squares represent the FM metallic sites and the white ones denote the PM insulating areas. The arrows indicate a warming process. As shown in Fig. 1, the system undergoes a transition from a FM state with few PM domains at low T to a PM state with few FM domains at high T,

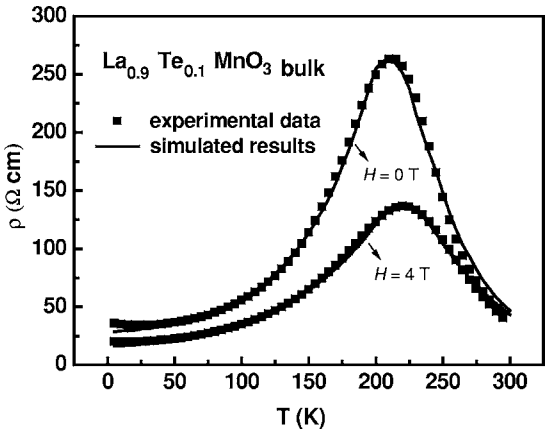

FIG. 2. Simulated T-dependent resistivity (solid lines) of $La_{0.9}Te_{0.1}MnO_3$ bulk compared with the experimental data (full circles) with and without H, respectively.

showing the mixed-phase characteristics when the FM to PM transition occurs. During warming, the size of the PM regions are nearly unchanged, except that the PM number is large enough to naturally connect those PM regions.

Based on the standard percolation description, the simulated results of the resistivity vs temperature (ρ-T) for $La_{0.9}Te_{0.1}MnO_3$ bulk are obtained, as shown in Fig. 2. The parameters A and B in the FM fraction f are set to be 0.009 and 1.22, respectively. The corresponding experimental data are also given in this figure, showing the MIT behavior accompanied with a FM to PM phase transition confirmed by electron spin resonance studies.[4,15] The simulated curves (solid lines) show an agreement with the experiment data, exhibiting the smooth MITs with and without H. After applying H, the magnetization of FM domains are aligned and the random spin disorder, especially around T_c, can be removed partially to cause a fraction of the insulating regions to convert into metallic regions.[5,12] Therefore, the resistivity is reduced and the MIT temperature T_{MI} is shifted from $\sim$210 K to a higher value of $\sim$220 K with H. The corresponding parameters used in simulation are listed in Table I with and without H. From Table I, we can see that the low T residual resistivity ρ_{m0} is reduced with H. It has been reported that the low T residual resistivity, ρ_{m0}, originates from scattering by impurities, defects, grain boundaries, and domain walls in the material.[14,27] We think the magnetic-field-induced motion of the domain walls can reduce those scatterings so that it can diminish the residual resistivity. In addition, we find that the electron-electron scattering coefficient ρ_{m1} and the magnon scattering coefficient ρ_{m2} are smaller than those without H, due to the fact that H reduces

TABLE I. Parameters used in the standard percolation simulation for $La_{0.9}Te_{0.1}MnO_3$ bulk with and without H, respectively.

H (T)	ρ_{m0} (Ω cm)	ρ_{m1} (Ω cm K^{-2})	ρ_{m2} (Ω cm K^{-4})	ρ_{i0} (Ω cm)	E_0/k_B (K)
0	25.34	1.50×10^{-3}	2.86×10^{-9}	0.18	1520
4	14.78	1.24×10^{-3}	0.45×10^{-9}	0.18	1470

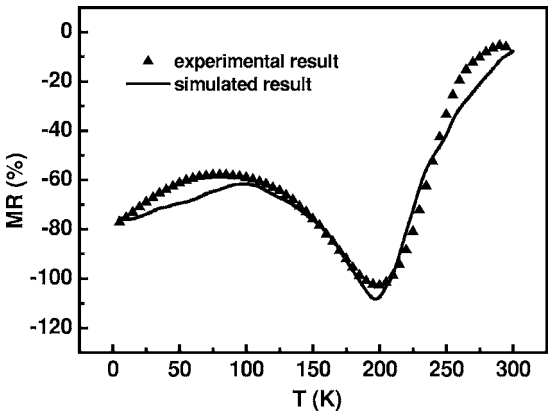

FIG. 3. The T-dependence MR of $La_{0.9}Te_{0.1}MnO_3$ bulk. Full triangles are the experimental data and the solid line is the calculated result obtained by the simulated results.

the spin scattering in conduction carriers by driving the local orientation of magnetization aligned.[6] Furthermore, the result reveals that H can induce the reduction of the activation energy E_0. The unchanged high T residual resistivity ρ_{i0} indicates that H does not reduce the resistivity of the PM components at very high T.

According to our simulated results, the magnetoresistance (MR), defined as $MR=[\rho(H)-\rho(0)]/\rho(H)$, where $\rho(H)$ and $\rho(0)$ are the resistivities with and without H, respectively, is plotted in Fig. 3 (solid line) for $La_{0.9}Te_{0.1}MnO_3$ bulk. The corresponding experimental results are represented by full triangles, showing a pronounced negative MR of $\sim -103\%$ at $T\sim 200$ K and displaying a CMR effect. The results indicate an approximate agreement between the experimental data and the simulated results, especially near the MIT.

However, standard percolation fails to obtain the abrupt change of resistivity near the transition when it is applied to the $La_{0.9}Te_{0.1}MnO_3$ thin film, as shown in Fig. 4 with dashed line. We introduce another percolation mode "cluster percolation," and this percolation process with the increased T is given in Fig. 5. Similarly, the small dark and white squares

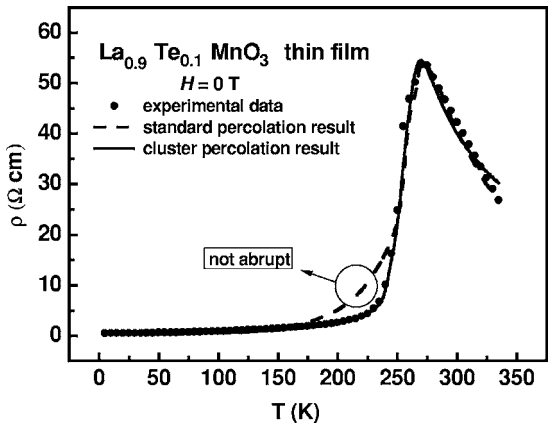

FIG. 4. Simulated result of the T-dependent resistivity obtained by cluster percolation (solid line) for $La_{0.9}Te_{0.1}MnO_3$ thin film without H. Full circles are the corresponding experimental data and the dashed line represents the simulated result obtained by standard percolation.

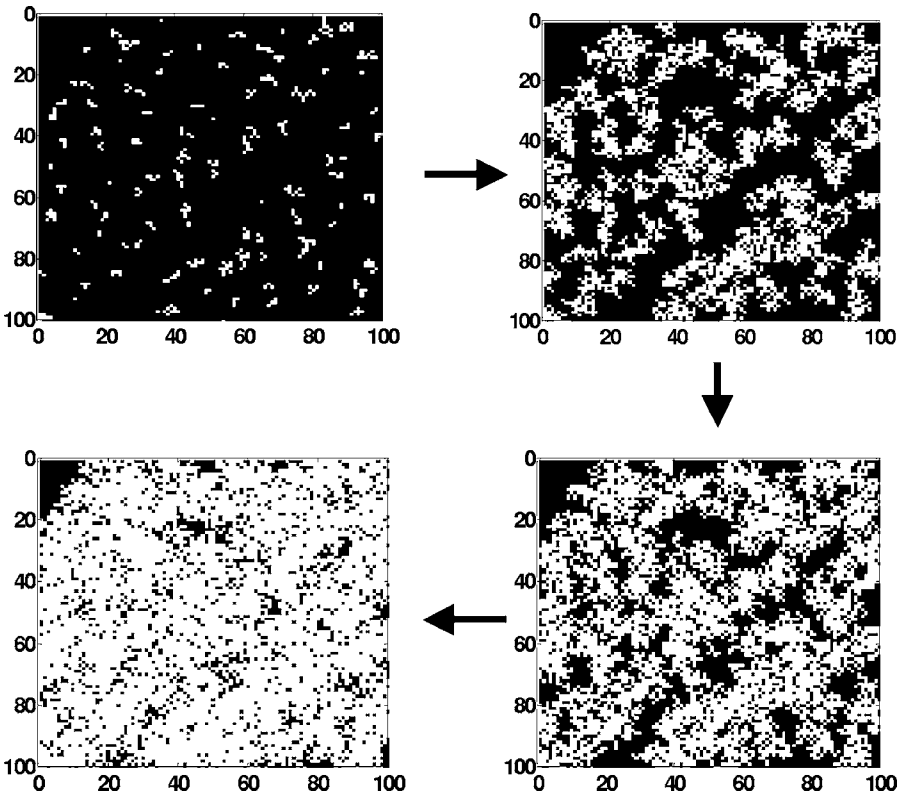

FIG. 5. Simulated process of cluster percolation from low-T FM (black) to high-T PM (white) phase transition in the mixed-phase description on a 100×100 matrix. The arrows indicate the warming process.

represent the FM metallic and PM insulating domains, respectively. The arrows indicate a warming process. It can be seen that the sizes of the PM domains can increase with T, but the number of the domains remains nearly unchanged. Further increasing T, these PM clusters will connect to each other and their number will decrease correspondingly, suggesting an abrupt change in resistivity. Based on the above cluster percolation description, the ρ-T curve of $La_{0.9}Te_{0.1}MnO_3$ thin film is obtained, as presented in Fig. 4 with a solid line. Full circles denote the corresponding experimental data. It can be seen that the simulated result obtained by the cluster percolation mode shows the abrupt character near the MIT. The above result indicates that the size of the PM domain in thin film increases with T. The corresponding parameters used are listed in Table II for $La_{0.9}Te_{0.1}MnO_3$ thin film in standard percolation and cluster percolation modes, respectively.

In order to further verify our assumption, we apply the cluster percolation scenario to the $La_{2/3}Ca_{1/3}MnO_3$ thin film deposited on the $SrTiO_3$ substrate to study its T-dependent resistivity property. It is well known that for the doping of $x \sim 1/3$, this material shows an MIT from low-T FM metallic phase to a high-T PM insulating phase. $La_{0.9}Te_{0.1}MnO_3$ materials and $La_{2/3}Ca_{1/3}MnO_3$ thin film are the different materials, so the difference of resistivity between their experimental data is rather remarkable. The experimental data of resistivity and the cluster percolation results are given in Fig. 6 for $La_{2/3}Ca_{1/3}MnO_3$ thin film. The parameters A and B in the FM fraction f are set to 0.019 and 1.0, respectively. To compare the difference between those two percolation

TABLE II. Parameters used in simulations for $La_{0.9}Te_{0.1}MnO_3$ thin film without H in standard percolation and cluster percolation modes, respectively.

Percolation mode	ρ_{m0} (Ω cm)	ρ_{m1} (Ω cm K^{-2})	ρ_{m2} (Ω cm K^{-4})	ρ_{i0} (Ω cm)	E_0/k_B (K)
Standard	0.26	2.14×10^{-5}	6.54×10^{-11}	1.5	860
Cluster	0.26	1.76×10^{-5}	4.90×10^{-11}	1.5	90

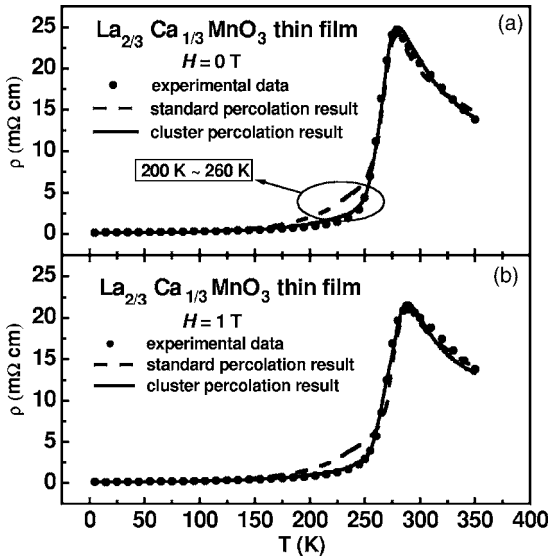

FIG. 6. Simulated T-dependent resistivities obtained by cluster percolation for $La_{2/3}Ca_{1/3}MnO_3$ thin film without (a) and with (b) H, respectively. Full circles are the corresponding experimental data and the dashed lines represent the simulated results obtained by standard percolation.

TABLE III. Parameters used in the cluster percolation simulation for $La_{2/3}Ca_{1/3}MnO_3$ thin film with and without H, respectively.

H (T)	ρ_{m0} (mΩ cm)	ρ_{m1} (mΩ cm K^{-2})	ρ_{m2} (mΩ cm K^{-4})	ρ_{i0} (mΩ cm)	E_0/k_B (K)
0	0.15	8.82×10^{-6}	2.45×10^{-11}	7.5	70
1	0.13	7.44×10^{-6}	1.75×10^{-11}	7.5	50

modes, we also give the simulated results using the standard percolation mode (dashed lines). Figure 6(a) shows the results of $La_{2/3}Ca_{1/3}MnO_3$ thin film without H. It can be seen that the results are similar to those of $La_{0.9}Te_{0.1}MnO_3$ thin film, presenting cluster percolation results in agreement with experimental data, while standard percolation cannot obtain the abrupt change in resistivity below the T_{MI}. After applying H, the resistivity is decreased, as presented in Fig. 6(b). The simulated results show that cluster percolation is also suitable for the $La_{2/3}Ca_{1/3}MnO_3$ thin film with H. Certainly, the corresponding coefficient parameters used in cluster percolation are changed compared with those without H, as listed in Table III. The changing rule of the parameters in cluster percolation is identical with that in standard percolation (see Table I). It should be noted that the H induced decrease of low-T residual resistivity in thin film is not remarkable compared with that in bulk, because the single crystal thin film with high quality has no obvious grain boundaries or defects different from the polycrystalline bulk. Those results further demonstrate that the abrupt transition in $La_{2/3}Ca_{1/3}MnO_3$ thin film can also be obtained by the cluster percolation mode rather than the standard percolation mode, indicating the domain size in thin film increases, but the domain number remains almost unchanged with the increased T. Figure 7 gives the curve of magnetization vs temperature with the magnetic field of 0.1 T parallel to the plane of the $La_{2/3}Ca_{1/3}MnO_3$ thin film. From Fig. 7, we can see that the highest resistivity ($\sim$280 K) corresponds to the occurrence of a large number of the PM components, which is identical with our transport model presented above.

From Fig. 6, we find that the main difference of the T-dependent resistivity lies in the temperature range of 200 K to 260 K. We present the simulated processes of phase transition without H from 200 K to 260 K for standard and cluster percolations, respectively, as plotted in Fig. 8. From the result of standard percolation process given in Fig. 8(a), we find that when T is increased to 260 K, the sizes of PM domains are slightly enhanced due to the large number of PM domains distributed in the system. Although some PM clusters begin to connect, there are still many separated PM domains with small sizes imbedded in the large-size FM clusters. Thus, the FM connecting paths still exist in this system, resulting in the small and smooth enhancement in the resistivity with the increased T. However, for the cluster percolation process, as shown in Fig. 8(b), many large-size PM domains almost connect at the same time when T is increased to 260 K. This connecting of PM clusters results in many separated FM clusters in the system. The FM connecting paths are rather rare, inducing a rapid enhancement in resistivity with the increased T.

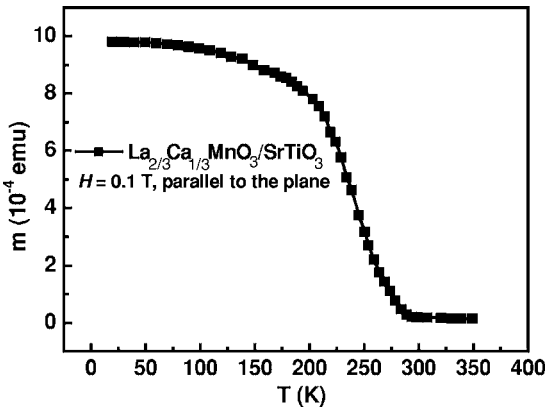

FIG. 7. The magnetic momentum of $La_{2/3}Ca_{1/3}MnO_3$ thin film versus temperature.

IV. DISCUSSION

On the basis of the above simulations, we find the abrupt character of resistivity in the thin films originates from the fact that the sizes of the PM insulating domains in thin film increase, but the cluster number remains unchanged with the increased T until those domain sizes are large enough to result in domain connection and decreased domain number. Furthermore, the size of cluster in thin film is correspondingly large compared with that of the bulk material. This characteristic is consistent with some experimental phenomena[5,9,10,12] and can be understood in the following ways.

Energetically, it is not convenient to create FM-PM interfaces and from this perspective it is energy-favorable to keep the number of FM-PM interfaces small by creating large clusters. A region first favoring an FM or PM state will nucleate at such a phase.[28] Hence, for the mixed-phase materials, the cluster percolation mode should be more rational than the standard percolation mode in general. We think that the standard percolation mode seems to work well for bulk material mainly because the crystal grain size limits the growing size of the mixed-phase domains. In our experiments, the $La_{0.9}Te_{0.1}MnO_3$ bulk is a polycrystalline material. A large number of random crystal grains in polycrystalline material results in many grain boundaries in bulk. With the increased temperature, to enlarge a PM domain around the grain boundaries, additional energy is required to overcome the grain boundaries, which is not energy favorable. On the contrary, as the $La_{0.9}Te_{0.1}MnO_3$ and $La_{2/3}Ca_{1/3}MnO_3$ thin films are single crystals without obvious grain boundaries, it is easy to enlarge the sizes of the PM clusters around those nucleated PM phases with the increased temperature. Therefore, it is preferable to form the large-scale domains in thin film, resulting in the abrupt change near the transition. Moreover, it has also been reported that a sample of $La_{0.7}Ca_{0.3}MnO_3$ with many small crystal grains has a very wide transition with a smooth change in resistivity, but a sample with no clear boundaries exhibits a narrow transition with a sharp change in resistivity,[29] which is consistent with our results. It can be concluded that the cluster percolation mode is necessary to describe the percolative transport of thin film.

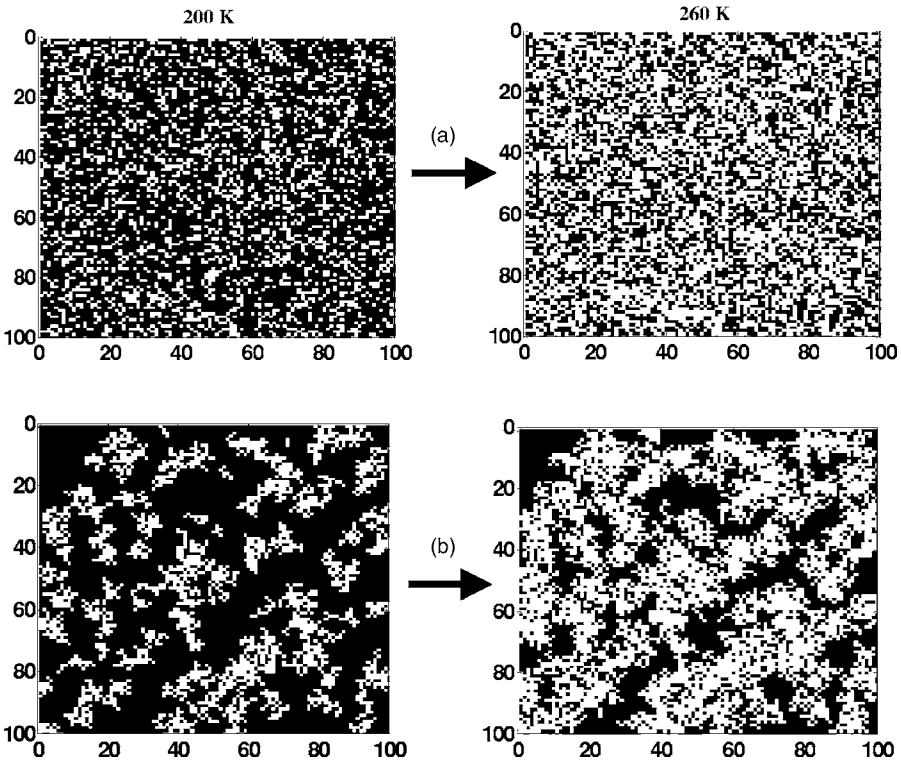

FIG. 8. Simulated process of phase transition from 200 K to 260 K on a 100×100 matrix obtained by standard percolation (a) and cluster percolation (b), respectively.

V. CONCLUSION

In summary, cluster percolation is introduced to explain the abrupt change near the MIT in thin film while standard percolation results in the smooth transition. After simulating the resistivity of the $La_{0.9}Te_{0.1}MnO_3$ bulk, $La_{0.9}Te_{0.1}MnO_3$ thin film, and $La_{2/3}Ca_{1/3}MnO_3$ thin film based on the phase separation theory, we find that cluster percolation is suitable for depicting the percolative conduction in thin film, indicating that the sizes of PM domains in thin film prefer to increase but the domain number is unchanged with the increased T. The agreement between the simulated results and our experimental data further shows that phase separation indeed lies in those studied materials and suggests that the intrinsic inhomogeneity plays a crucial role in the electrical conductivity and the CMR effect. Moreover, it is revealed that the size of the crystal grains in bulk may have a significant influence on the size of the coexisting clusters, resulting in the larger domain size in thin film than that in bulk.

ACKNOWLEDGMENT

We acknowledge the financial support from the National Natural Science Foundation of China.

*Corresponding author. Fax: 86-10-82648099. Email address: kjjin@aphy.iphy.ac.cn

[1] S. Jin, T. H. Tiefel, M. MacCormack, R. A. Fastnacht, R. Ramesh, and L. H. Chen, Science **264**, 413 (1994); Kui-juan Jin, Hui-bin Lu, Qing-li Zhou, Kun Zhao, Bo-lin Cheng, Zhenghao Chen, Yue-liang Zhou, and Guo-Zhen Yang, Phys. Rev. B **71**, 184428 (2005); Hui-Bin Lu, Kui-Juan Jin, Yan-Hong Huang, Meng He, Kun Zhao,Bo-Lin Cheng, Zheng-Hao Chen, Yue-Liang Zhou, Sou-Yu Dai, and Guo-Zhen Yang, Appl. Phys. Lett. **86**, 241915 (2005); Kun Zhao, Yanhong Huang, Qingli Zhou, Kui-Juan Jin, Huibin Lu, Meng He, Bolin Cheng, Yueliang Zhou, Zhenghao Chen, and Guozhen Yang, *ibid.* **86**, 221917 (2005).

[2] M. R. Ibarra and J. M. De Teresa, J. Magn. Magn. Mater. **177-181**, 846 (1998).

[3] S. L. Yuan, W. Y. Zhao, G. Q. Zhang, F. Tu, G. Peng, J. Liu, Y. P. Yang, G. Li, Y. Jiang, X. Y. Zeng, C. Q. Tang, and S. Z. Jin, Appl. Phys. Lett. **77**, 4398 (2000).

[4] G. T. Tan, S. Dai, P. Duan, Y. L. Zhou, H. B. Lu, and Z. H. Chen, Phys. Rev. B **68**, 014426 (2003).

[5] M. Uehara, S. Nori, C. H. Chen, and S. W. Cheong, Nature (London) **399**, 560 (1999).

[6] Y. Tomioka, A. Asamitsu, H. Kuwahara, Y. Moritomo, and Y. Tokura, Phys. Rev. B **53**, R1689 (1996).

[7] C. Zener, Phys. Rev. **82**, 403 (1951).

[8] A. J. Millis, Nature (London) **392**, 147 (1998).

[9] J. M. De Teresa, M. R. Ibarra, P. A. Algarabel, C. Ritter, C. Marquina, J. Blasco, J. García, A. del Moral, and Z. Arnold, Nature (London) **386**, 256 (1997).

[10] L. Zhang, C. Israel, A. Biswas, R. L. Greene, and A. de Lozanne, Science **298**, 805 (2002).

[11] M. Cavallini, and F. Biscarini, Rev. Sci. Instrum. **71**, 4457 (2000); C. Albonetti, I. Bergenti, M. Cavallini, V. Dediu, M. Massi, J.-F. Moulin, and F. Biscarini, *ibid.* **73**, 4254 (2002).

[12] M. Fäth, S. Freisem, A. A. Menovsky, Y. Tomioka, J. Aarts, and J. A. Mydosh, Science **285**, 1540 (1999).
[13] X. T. Zeng and H. K. Wong, Appl. Phys. Lett. **72**, 740 (1998); V. S. Amaral, A. A. C. S. Lourenco, J. P. Araújo, A. M. Pereira, J. B. Sousa, P. B. Tavares, J. M. Vieira, E. Alves, M. F. da Silva, and J. C. Soares, J. Appl. Phys. **87**, 5570 (2000); H. S. Choi, W. S. Kim, B. C. Nam, and N. H. Hur, Appl. Phys. Lett. **78**, 353 (2001); G. T. Tan, X. Zhang, and Z. H. Chen, J. Appl. Phys. **95**, 6322 (2004).
[14] R. Mahendiran, S. K. Tiwary, A. K. Raychaudhuri, T. V. Ramakrishnan, R. Mahesh, N. Rangavittal, and C. N. R. Rao, Phys. Rev. B **53**, 3348 (1996); R. W. Li, J. R. Sun, Z. H. Wang, S. Y. Zhang, and B. G. Shen, J. Phys. D **33**, 1982 (2000).
[15] G. T. Tan, S. Y. Dai, P. Duan, Y. L. Zhou, H. B. Lu, and Z. H. Chen, J. Appl. Phys. **93**, 5480 (2003).
[16] M. Mayr, A. Moreo, J. A. Vergés, J. Arispe, A. Feiguin, and E. Dagotto, Phys. Rev. Lett. **86**, 135 (2001).
[17] J. Burgy, E. Dagotto, and M. Mayr, Phys. Rev. B **67**, 014410 (2003).
[18] D. Stauffer, *Introduction to Percolation Theory* (Taylor & Francis, London and Philadelphia, 1985).
[19] Qing-li Zhou, Kui-juan Jin, Dong-yi Guan, Zheng-hao Chen, Huibin Lu, and Guo-zhen Yang, Phys. Lett. A (to be published).
[20] S. Ju, H. Sun, and Z. Y. Li, J. Phys.: Condens. Matter **14**, L631 (2002).
[21] S. Kirkpatrick, Rev. Mod. Phys. **45**, 574 (1973).
[22] A. H. Thompson, Phys. Rev. Lett. **35**, 1786 (1975).
[23] K. Kubo and N. Ohata, J. Phys. Soc. Jpn. **33**, 21 (1972).
[24] S. L. Yuan, W. Y. Zhao, G. Q. Zhang, F. Tu, G. Peng, J. Liu, Y. P. Yang, G. Li, Y. Jiang, X. Y. Zeng, C. Q. Tang, and S. Z. Jin, Appl. Phys. Lett. **77**, 4398 (2000).
[25] A. K. Pradhan, Y. Feng, B. K. Roul, and D. R. Sahu, Appl. Phys. Lett. **79**, 506 (2001).
[26] S. Skiena, *Implementing Discrete Mathematics: Combinatorics and Graph Theory with Mathematica* (Addison-Wesley, California, 1990).
[27] H. Huhtinen, R. Laiho, K. G. Lisunov, V. N. Stamov, and V. S. Zakhvalinskii, J. Magn. Magn. Mater. **238**, 160 (2002); A. Gupta, G. Q. Gong, Gang Xiao, P. R. Duncombe, P. Lecoeur, P. Trouilloud, Y. Y. Wang, V. P. Dravid, and J. Z. Sun, Phys. Rev. B **54**, R15629 (1996); S. Pignard, H. Vincent, J. P. Sénateur, K. Fröhlich, and J. Šouc, Appl. Phys. Lett. **73**, 999 (1998).
[28] E. Dagotto, T. Hotta, and A. Moreo, Phys. Rep. **344**, 1 (2001).
[29] X. L. Wang, S. X. Dou, H. K. Liu, M. Lonescu, and B. Zeimetz, Appl. Phys. Lett. **73**, 396 (1998).